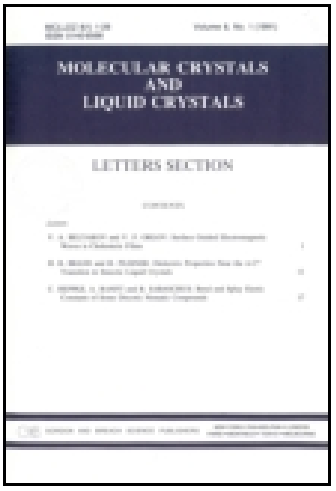

Molecular Crystals and Liquid Crystals
Publication details, including instructions for authors and subscription information:
http://www.tandfonline.com/loi/gmcl20

Nonlinear Optics of Nematic and Blue Phase Liquid Crystals

Iam Choon Khoo[a], Chun-Wei Chen[a], Kuan Lung Hong[a], Tsung-Hsien Lin[a] & Shuo Zhao[a]

[a] Department of Electrical Engineering, Pennsylvania State University, University Park, PA

Published online: 30 Sep 2014.

To cite this article: Iam Choon Khoo, Chun-Wei Chen, Kuan Lung Hong, Tsung-Hsien Lin & Shuo Zhao (2014) Nonlinear Optics of Nematic and Blue Phase Liquid Crystals, Molecular Crystals and Liquid Crystals, 594:1, 31-41, DOI: 10.1080/15421406.2014.917469

To link to this article: http://dx.doi.org/10.1080/15421406.2014.917469

Mol. Cryst. Liq. Cryst., Vol. 594: pp. 31–41, 2014

ISSN: 1542-1406 print/1563-5287 online
DOI: 10.1080/15421406.2014.917469

Taylor & Francis
Taylor & Francis Group

Nonlinear Optics of Nematic and Blue Phase Liquid Crystals

IAM CHOON KHOO,* CHUN-WEI CHEN, KUAN LUNG HONG, TSUNG-HSIEN LIN, AND SHUO ZHAO

Department of Electrical Engineering, Pennsylvania State University, University Park, PA

We present a critical reexamination of individual electronic and collective optical nonlinearities of nematic liquid crystals (NLC) in the context of all-optical transmission switching of femtoseconds – CW lasers, and report recent observations of similar optical nonlinearities in Blue-phase liquid crystals (BPLC) and their utilization in feasibility demonstrations of polarization-free nonlinear grating diffraction and transmission switching of CW as well as pulsed lasers.

Keywords Optical nonlinearities; blue-phase; nematic; nonlinear grating diffractions; femtoseconds; nanoseconds and microseconds all-optical switching; fiber array

1. Nonlinear Optics of Nematics – Merits and Limitations

Among the mesophases of liquid crystals, nematic liquid crystals (NLC) are the most frequently investigated for their nonlinear-optical responses [1, 2]. In general, they possess two types of optical nonlinearities: (i) ultrafast "electronic" optical nonlinearities arising from individual molecular resonant interaction with the optical electric field, with corresponding nonlinear macroscopic susceptibilities $\chi^{(2)}$, $\chi^{(3)}$, ... etc.; (ii) "non-resonant" collective optical nonlinearities associated with laser-induced collective crystalline axes alignment or reorientation, order parameter changes due to thermal and density fluctuations, and other mechanisms unique to the liquid crystalline ordered phases.

Individual molecular optical nonlinearities of NLC are similar to other organic molecules [3], and arise from the optical field induced nonlinear polarizations associated with multi-photonic transitions amongst the ground and excited states of the molecules, c.f. Fig. 1. Since bulk nematic liquid crystals (NLC) are centro-symmetric, the first non-vanishing nonlinear polarization term is cubic in the optical electric field, $P^{(3)} \sim \chi^{(3)}EEE$ where $\chi^{(3)}$ is the complex third order nonlinear susceptibility. This term is responsible for various optical self-action and wave mixing processes. Perhaps the most frequently investigated nonlinear optical response is the polarization $P^{(3)} \sim \chi^{(3)}(EE^*)E$ that corresponds to an intensity dependent refractive index change $\Delta n \sim \chi_{Rl}{}^{(3)}(EE^*) = n_2 I$; here $\chi_{Rl}{}^{(3)}$ is the real part of $\chi^{(3)}$, E the optical electric field and I the optical intensity and n_2 is the nonlinear index coefficient. Typical liquid crystals molecular off-resonant n_2 value is on the order of $\sim 10^{-14}$ cm^2/W, and could be larger near electronic or structural resonances [3–6]. Because

*Address correspondence to ick1@psu.edu

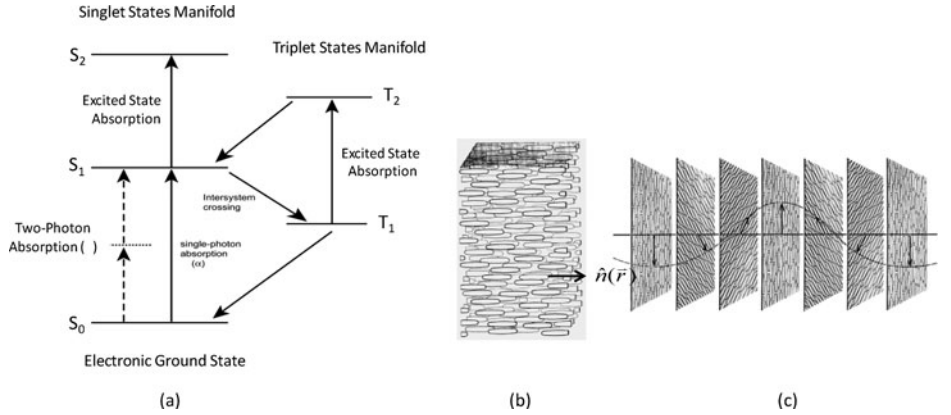

Figure 1. (a) Typical molecular energy level structure of LC molecule that possesses strong two-photon transition (at the wavelength of interest) from the ground state to excited singlet states which could make intersystem crossing to excited triplet states. (b) Director axis arrangement in nematic liquid crystal; (c) chiral nematic (cholesteric) liquid crystal where the director axis spirals around with a pitch on the order of optical wavelength.

of their ultrafast response, such intensity dependent index change can be employed for various femtoseconds phase-modulation and pulse-compression application [6].

On the other hand, the imaginary part of $\chi^{(3)}$ comes from multi-photon absorption processes. In general, NLC molecules possess sizeable nonlinear absorption coefficients due to their organic molecular constituents [3–5]. For example, the intrinsic two-photon absorption coefficients β_{int} of transparent liquid crystal molecules are on the order 0.4 cm/GW measured with femtoseconds laser pulses. With contribution from excited state absorptions and intersystem singlet-triplet crossing at longer time scales, the resulting effective nonlinear absorption coefficients β_{eff} are generally much larger than their intrinsic values, ranging from $\sim$ 4 cm/GW to over 25 cm/GW in studies conducted with picoseconds – nanoseconds pulsed lasers [4, 5]. These nonlinear absorption coefficients have been employed for highly effective large-dynamic-range optical limiting action against femtoseconds – nanoseconds lasers [7–9].

In their ordered phases, the director axis of the liquid crystal self-assembles in many configurations; Fig. 1b & 1c depict typical arrangement found in the nematic and cholesteric phase. The collective optical nonlinearities of nematic liquid crystals associated with director axis reorientation are extraordinarily large, due mainly to the large birefringence of nematics and the ease with which the director axis or the order parameter can be perturbed by the optical field [1, 2]. Studies conducted over the years have yielded nonlinear index coefficients of magnitudes ranging from 10^{-4} cm^2/W in undoped NLC to well over 1000 cm^2/W in NLC containing dye- or other dopants [1, 2, 10–12]. As a result, almost all conceivable nonlinear optical phenomena have been observed, with lasers of wide-ranging power, spectral and temporal characteristics [1, 2, 11]. Due to their fluid nature, NLC have also been incorporated in a multitude of non-planar structures or tightly confined structures such as micro-resonator, photonic crystals, holey fibers, waveguides and plasmonic-metamaterials and -nanostructures to enable dynamical control of refractive index, light transmission, spectral reflection, polarization states, beam shape and direction, and other characteristics [13–21].

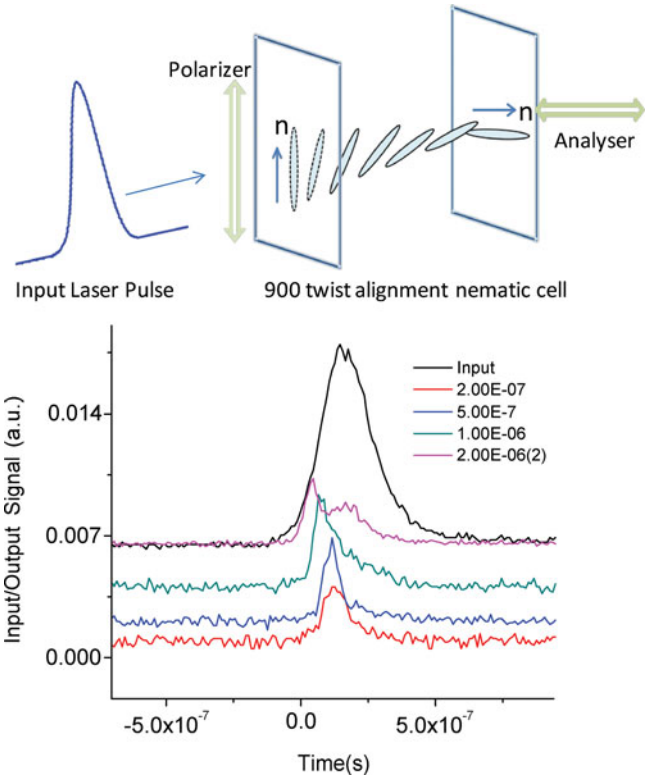

Figure 2. Upper figure: 90° twist alignment NLC cell placed between two crossed polarizers for self-action switching. Lower figure: Oscilloscope traces of input and transmitted output laser pulses through a IR dye-doped 5CB sample for various input laser pulse energies. Laser wavelength: 750 nm; LC thickness: 200 μm; laser spot size: 140 μm.

Besides director reorientation nonlinearities with relaxation times on the order of milliseconds, NLC also possess faster optical nonlinearities associated with laser-induced thermal, density, order parameter and coupled flow-reorientation processes [11, 22, 23]. These nonlinearities have been employed for optical wave mixing, modulations, tuning and switching operations at microseconds – nanoseconds speed. An exemplary optical switch is depicted in Fig. 2 -consisting of a 90-degree twist-alignment nematic cell sandwiched between two crossed polarizers. In electro-optical switching operation, the transmission of the cell is controlled by an applied AC electric field between the two cell walls or across in-plane electrodes to realign the director axis, thereby changing the polarization state of the light in traversing the cell and the transmission through the exit polarizer. On the other hands, in nonlinear or all-optical switching, the intensity/field of the incident light would reorient or randomize the director axis to affect its transmission through the output polarizer [11, 24–26]. Actual switching speed depends on specific interaction geometries and the actual nonlinear mechanism(s) involved, as well as the temporal characteristics and intensity of the laser. For characteristics diffusion lengths in the microns range and typical nematogen parameters, the density and thermal relaxation time constants are on the order of nanoseconds to microseconds [1, 2, 11]. Accordingly, if the initial portion of a laser

pulse can build up sufficiently birefringence changes in a time shorter than these relaxation times, the later portion of the pulse will experience diminished transmission.

Figure 2 shows results obtained with a near-infrared dye-doped NLC cell. A single linearly polarized laser pulse from the q-switched laser system ($\lambda = 750$ nm; pulse duration = 250 ns) is focused into the 90° twist alignment NLC cell and the output pulse is detected and its time evolution is recorded by a fast oscilloscope. At low input pulse energies, the NLC is essentially not perturbed; the laser polarization vector follows the spatial twisting of the director axis, and is linearly transmitted through the output polarizer with the same pulse shape. At input laser energies above 0.5 μJ, the later portion of the pulse begins to exhibit lower transmission. The time it takes to begin such switch-off shortens as the input energy is increased from 0.5 μJ to 2 μJ, consistent with the theoretical modeling based on laser induced heating and order parameter changes [24]. The extinction ratio obtained with this all-optical self-action switch can be quite high (∼1000), and the switch-off time can be as short as 50 ns [24–26]. These non-resonant optical nonlinearities of nematics are also relatively insensitive to the optical frequency, and can therefore be utilized throughout the visible-infrared spectrum [1, 2, 11].

Nevertheless, it is important to note here that NLC do possess some inherent drawbacks that invariably lead to less than optimal performance in practice. First is the omnipresent surface alignment layer to provide strong anchoring forces needed to induce bulk ordering. Strong anchoring inevitably results in establishing a practically immobile liquid crystal layer which do not respond to applied field or short-range plasmonic field from LC-plasmonic nanostructures or plasmonic nano-particles suspended in bulk NLC. Consequently, in almost all experimental studies of optical tuning/modulation of such NLC systems, one tends to observe higher threshold and/or much smaller tuning range, modulation depth . . . etc. and [15–20]. Another inherent drawback of nematic is the need for polarized light; this imposes many restrictive conditions on practical application, especially in non-planar NLC-Plasmonic structures for waveguides, metamaterials or transformative optics [13–21].

2. Blue Phase Liquid Crystals as Next Generation Nonlinear Optical Materials

To circumvent these nematic limitations, we have conducted several studies [27–30] on Blue Phase Liquid Crystals (BPLC) and also Polymer-Stabilized Blue phase liquid crystals (PS-BPLC) [31–34]. In BPLC, the molecules self-assemble into tightly wound defect-spirals that form 3-D cubic or BCC lattices c.f. Fig. 3. Because the lattice constants are smaller than visible wavelength, bulk BPLC's are optically isotropic, unlike the highly birefringent NLC, or cholesteric liquid crystals (CLC) which reflect/transmit circularly polarized lights [35,36]. Furthermore, owing to the tightly confined director axis arrangement, *scattering loss and relaxation times of BPLC's are greatly reduced*. This allows high transmission through much longer path lengths, and the generation of large phase shift with much lower threshold power requirement and faster response times than nematic.

The BPLC mixture used in our studies consists of a chiral dopant (Merck S-811) dissolved in a nematic host (E48 & 5CB) with a positive dielectric anisotropy in the ratio: E48(32%):5CB(32%):S811(36%)]. This material exhibits a Blue-Phase temperature range of ∼9°C with the following phase sequence during cooling from the isotropic phase: Blue-Phase II (below 31°C) and Blue Phase I (below 29°C), and the focal conic cholesteric phase (below 22°C). In polymer-stabilized blue phase liquid crystals [See ref. 28 or 30 for

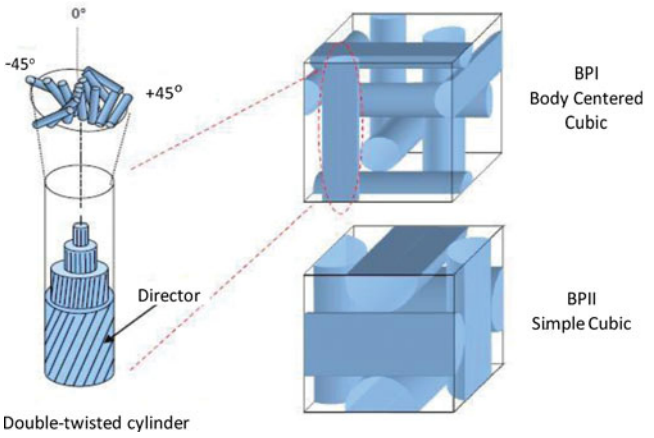

Figure 3. Double helix arrangement of the BPLC director axis and the body-centered cubic and simple cubic crystal lattice structures corresponding to the BPI and BPII phases

preparation procedure], a typical phase sequence is: Iso-(56.2°C)-BP-(<0°C)-N, i.e. the temperature range of BPLC is more than 56°C in this case.

2.1. Nonlinear Grating Diffractions with CW and Pulsed Lasers in Planar BPLC Cells

Our first study [27] of BPLC's nonlinear optical response was conducted with an optical grating diffraction set up depicted in Fig. 4. We have studied undoped BPLC and BPLC lightly doped with Methyl-Red (MR) dye (<1%, corresponding to an absorption constant of $\sim$20 cm^{-1} measured in the isotropic liquid phase). These BPLC are introduced into cells made with clean but untreated glasses. A linearly polarized laser ($\lambda = 532$ nm) is split into two coherent beams which are then overlapped on the BPLC sample at a small wave mixing angle, with the polarization state of these pump beams being parallel or orthogonal to each other.

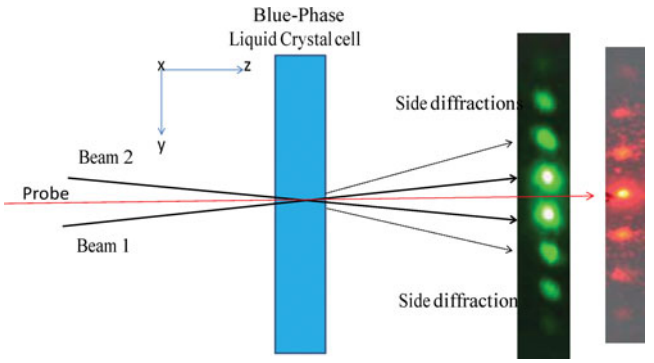

Figure 4. Nonlinear self- and probe-beam diffraction experimental set up for characterizing the nonlinear index coefficient of BPLC using pump lasers ($\lambda = 532$ nm) and probe ($\lambda = 632.8$ nm). Photos to the right show the transmitted beam and various side diffraction orders.

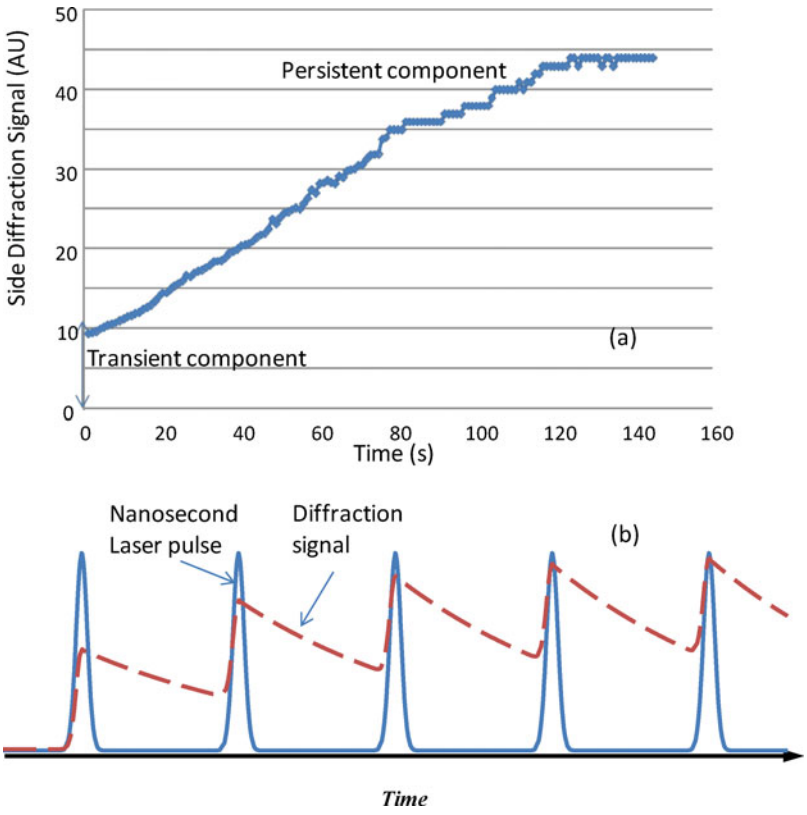

Figure 5. (a) Dynamical evolution of the first order diffraction signal from MR-doped BPLC cell illuminated by an optical intensity grating, exhibiting an initial fast build-up transient component and a slow build-up persistent component. Sample thickness: 100 μm; laser power: 22 mW; beam spot diameter: 3 mm, wave mixing angle $\theta = 0.012$ rad.; grating spacing $\Lambda \sim 66$ μm (b) Schematic depiction of side-diffraction signal build up by repetitively pulsed nanoseconds pump-lasers. Time interval between pulses is not drawn to scale.

With CW pump lasers, side diffractions are observed from the dye-doped sample; the full details regarding the self-diffractions build-up and possible contributing mechanisms can be found in [27]. Essentially, under low power illuminations, only the first-order side-diffraction appears and it starts off as a transient component c.f. Fig. 5a. The magnitude of this component depends on the concentration of the dye-dopant; the higher is the concentration, the larger is its magnitude. This component is attributed to the thermal grating resulting from photo-absorption by the MR dye dopant. The observed relaxation time of this transient component is on the order of several milliseconds for the grating constant of $\sim$60 μm, which is consistent with typical thermal grating relaxation dynamics of the nematic host in BPLC [1–3].

Upon prolonged illumination, the self- and probe- diffractions continue to *build up*, and second-, third- and higher-order self-diffractions begin to appear, eventually reaching a steady state in a minute or so, c.f. Fig. 5(a). This slow build-up component acquires a persistent nature; when the pump-beams are turned off, they decay in 10's minutes. They can be completely erased, however, by simply heating the sample to the isotropic liquid

state. This persistent component is attributed to laser induced lattice distortion mediated by the migration of photo-excited dye dopant molecules. The observed nonlinear index coefficient n_2 is on the order of -4.3×10^{-4} cm^2/Watt for a grating spacing of $\sim$66 μm; with larger grating constant or thicker sample, n_2 values can approach 10^{-3} cm^2/Watt. By comparison, the much weaker transient thermal index component corresponds to an n_2 value of $\sim -10^{-5}$ cm^2/W typical of NLC [1, 3]. We have repeated the experiments with BPLC doped with other absorbing azo-dyes [Beam Corporation], and observed analogous side diffraction results. It is important to point out here that the build-up of the persistent component *can be observed only in the BPI or BPII phase*. If the dopant concentration is too high, the resulting thermal heating tends to drive the system into the isotropic phase when only a weak transient thermal grating component would manifest.

We have also verified the isotropy of BPLC's nonlinear optical response by varying the direction of incidence of the pump beams on the sample, and also the orientation of the pump laser polarizations. No observable diffraction is detected in all samples illuminated by pump beams with orthogonal polarizations up to the highest power available from our laser systems. Diffractions are produced by pump beams of parallel polarizations, i.e. an optical intensity grating; no appreciable difference in the magnitude or dynamics of the self- or probe-diffractions are detected as we vary the sample orientation with respect to the intensity grating wave vector. Also, the polarization state of the diffractions always follows that of the probe.

As a further probe of BPLC's nonlinear optical response, we have recently performed similar grating diffraction experiments on undoped BPLC using high power pulsed laser ($\lambda = 532$ nm; pulse duration $\tau_p = 10$ ns; pulse rate variable from single-shot to 10 pps; beam spot size $\sim$200 μm). Side diffractions begin to manifest with laser pulse energy above $\sim$200 μJ. Under such intensity, possible contributing mechanisms are electrostriction or Maxwell Stress induced flow-reorientation as well as thermal/density effects [22, 23] following multi-photon absorptions by the nematic constituents in BPLC as they possess significant two- and multiple-photon absorption cross-sections at the 532 nm spectral region. The electrostriction or Maxwell Stress from the intense laser field is responsible for the observation of a transient weak diffraction signal in single-shot experiment. On the other hand, under prolonged illumination by repetitively pulsed lasers, the diffraction is observed to build up by the succession of pump pulses, c.f. Fig. 5b, and eventually acquire a persistent component due to the thermal/density lattice distortion effects similar to those produced by a CW laser.

2.2. Nonlinear Transmission with BPLC Fiber Array and Random Lasing

Because of the polarization independence and freedom from surface alignment requirement, BPLC's are ideal for filling capillary array to fabricate optical fiber array similar to our previous work [7–9] with isotropic organic liquid c.f. Fig. 6. These BPLC fiber arrays are capable of high-resolution image transmission just as other isotropic liquid cored fiber arrays; however, because of the 3-D photonic crystal properties of the BPLC cores, they exhibit tunable photonic bandgaps (reflection/transmission bands) not possible with their isotropic-liquid-cored counterparts. Our studies with a CW picoseconds continuum laser have also demonstrated all-optical transmission switching enabled by the nonlinear mechanisms occurring in the BPLC guiding core. These mechanisms include multi-photon absorptions of the BPLC constituent molecules, (negative) thermal index change that lead to defocusing and loss of guiding mode similar to other organic liquid cored fiber array [7–9].

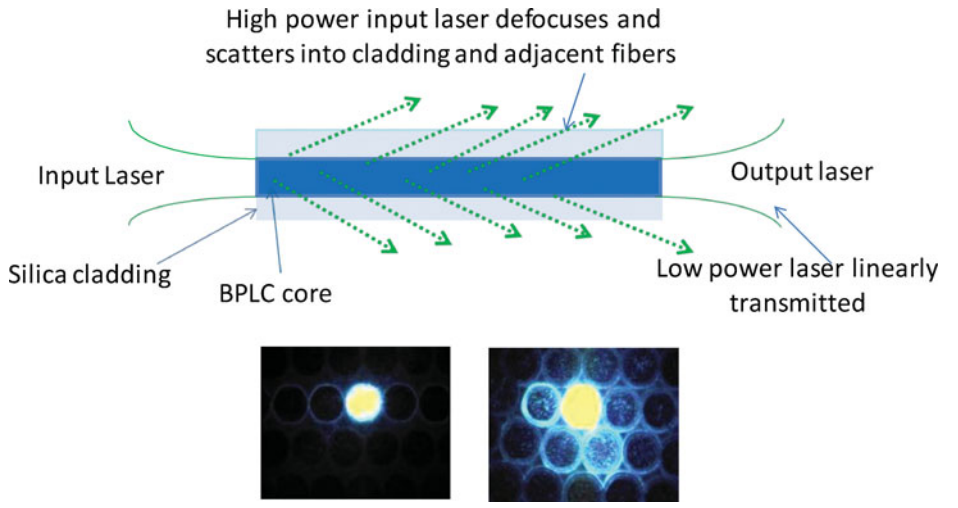

Figure 6. Schematic depiction of the transformation of a core-guided low power laser to side-scattered cladding mode when the laser power is high enough to create negative index change, defocusing effect and loss of guiding core transmission.

We have recently conducted further studies of the dynamics of the defocusing effects caused by laser induced thermal/density changes in BPLC. As depicted in Fig. 7, a pump laser ($\lambda = 532$-nm) of 20 nanoseconds pulse-duration and a collinear CW He-Ne probe laser ($\lambda = 632.8$ nm) are focused (spot diameter $\sim$200 μm) onto a 1mm-thick undoped BPLC cell maintained in the BPII phase; a planar cell is used here instead of fiber in order to avoid complication/contribution arising from the core-cladding interface. At input

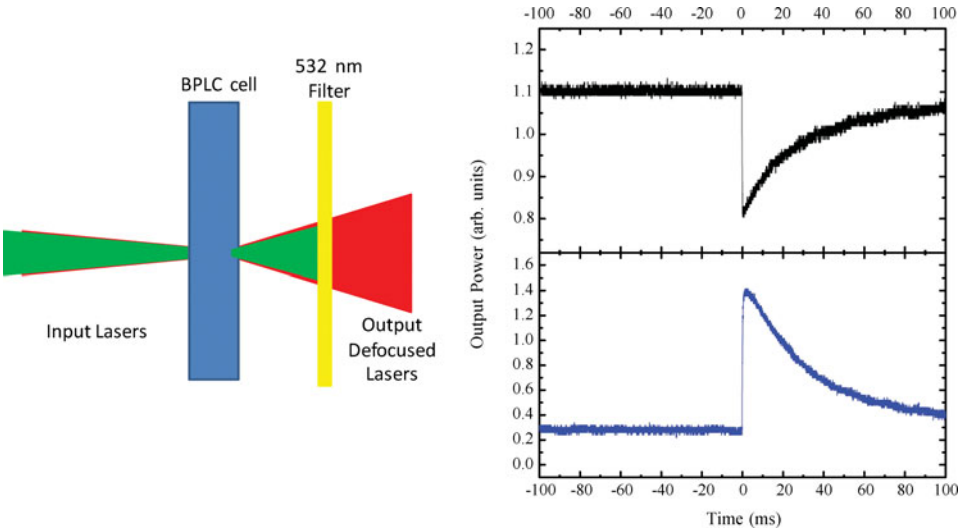

Figure 7. Nanosecond laser induced defocusing effect with 1 mm-thick undoped BPLC: (a) Laser power in the central portion of the transmitted probe beam; (b) Laser power in the off-axis part of the transmitted probe beam.

pulse energy above 200 μJ, the transmitted lasers exhibits obvious defocusing effect; the central region of the transmitted beams darkens while the beam divergence increases. Fig. 7a & b inserts show the detected on-axis and off-axis beam power of the transmitted He-Ne probe following the pump pulse. Due to the ns laser induced defocusing effect, the on axis region exhibits an abrupt drop in intensity while the side region experiences an abrupt rise. These are followed by a slow return to their respective original levels. The initial drop/rise change occur in $\sim$400 μs, while the subsequent return to original takes $\sim$100 ms. These dynamical behaviours are analogous to those thermal/density effects observed with pulsed lasers in NLC [11, 22, 23], which are expected since they are the main constituents of BPLC. Accordingly, these BPLC cells or fiber arrays could be utilized for similar all-optical transmission switching of microseconds-nanoseconds lasers.

With laser-dye doped BPLC and polymer-stabilized BPLC (PS-BPLC) filled capillaries, we have also demonstrated the feasibility of producing controllable random lasers [28]. Such lasers possess many useful characteristics, and have been observed in various host media including nematic or cholesterics liquid crystals [37–40]. Blue-Phase liquid crystals (BPLC) with their 3-D photonic crystalline make-up, optical isotropy (polarization independence), much faster electro-optics response than nematic, and ease of fabrication as they generally do not require surface alignment, are in many respects more desirable than cholesterics or nematics as the laser host media.

3. Concluding Remarks

We have presented a brief review of the optical nonlinearities of nematic liquid crystals and their ultrafast all-optical switching possibilities, and reexamined their merits and limitations Our recent nonlinear grating studies have demonstrated that under cw laser illumination, dye-doped BPLC possess giant polarization-insensitive optical nonlinearities with intensity dependent nonlinear index coefficients that can be as large as 10^{-3} cm^2/W. With more intense nanoseconds – picoseconds pulse excitation, undoped BPLC also exhibit fast-responding nonlinear optical effects associated with laser induced thermal/density effects that relax in sub-microseconds to nanoseconds regime, similar to NLC. Since the nematic molecular constituents of BPLC possess large two-photon and excited-state absorption efficiencies, they are therefore also promising alternatives for ultrafast (picoseconds - femtosecond) nonlinear transmission and pulse compression applications. Efforts are currently underway to quantitatively characterize these mechanisms over the vast time scale spanning femtoseconds to microseconds with the aim of establishing BPLC as a polarization-free alternative to NLC and CLC for next generation photonics applications.

Acknowledgments

We gratefully acknowledge support by the Air Force Office of Scientific Research. All authors are in Pennsylvania State University when the work is performed.

References

[1] Khoo, I. C. (2009). *Physics Report*, *471*, 221–267.
[2] Khoo, I. C. (2011). *J. Opt. Soc. Am.*, *B28*, A45–A55.
[3] Christodoulides, D. N., Khoo, I. C., Salamo, G. J., Stegeman, G. I., & Van Stryland, E. W. (2010). *Adv. Opt. Photon.*, *2*, 60–200.

[4] Khoo, I.C., Webster, S., Kubo, S., Youngblood, W. J., Liou, J., Diaz, A., Mallouk, T. E., Lin, P., Peceli, D., Padilha, L. A., Hagan, D. J., & Van Stryland, E. W. (2009). *J. Mater. Chem.*, *19*, 7525–7531.
[5] Khoo, I. C., & Diaz, A. (2011). *J. Opt. Soc. Am.*, *B28*, 1702–1710 and references therein.
[6] Song, Liyan., Fu, Shenhe, Liu, Yikun, Zhou,*, Jianying, Chigrinov, Vladimir G. , & Khoo, I. C. (2013). *Optics Letters*, *38*, 5040–5042
[7] Khoo, I. C. (2008) *IEEE J. Selected Topics in Quantum Electronics JSTQE 14, no. 3*, 946–951
[8] Khoo, I.C., Diaz, Andres & Ding, J. (2004). *J. Opt. Soc. Am*, *B21*, 1234–1240.
[9] Khoo, I. C. & Li, H., (1994). *Appl. Phys.*, *B59*, 573–580.
[10] Khoo, I.C., Slussarenko, S., Guenther, B. D. & Wood, W. V. (1998). *Opt. Letts*, *23*, 253–255.
[11] Khoo, I. C. (2014). *Progress in Quantum Electronics* Vol. *38*, Issue 2, 77–117.
[12] Khoo, I. C. (1996). *Mol. Cryst. Liq. Cryst*, *282*, 53–66 and references therein.
[13] Wang, X., Kwon, D. H., Werner, D. H., Khoo, I. C., Kildishev, A. & Shalaev, V. M. (2007). *Appl. Phys. Lett. 91*, 143122.
[14] Bossard, J. A., Liang, X., Li, L., Werner, D. H., Weiner, B., Cristman, P. F., Diaz, A., & Khoo, I. C. (2008), *IEEE Transactions on Antennas and Propagation*, *56*, pp. 1308–1320 (2008).
[15] Pawlik, G., Tarnowski, K., Walasik, W., Mitus, A.C. and Khoo, I.C. (2012). *Optics Letters 37*, 1847–1849.
[16] Xiao, Shumin, Chettiar, Uday K., Kildishev, Alexander V., Drachev, Vladimir, Khoo, I. C., & Shalaev, Vladimir M. (2009). *Appl. Phys. Lett.*Vol. *95* Iss: 3, Article Number: 033115.
[17] Minovich, Alexander, Farnell, James, Neshev, Dragomir N., McKerracher, Ian, Karouta, Fouad, Tian, Jie, Powell, David A., Shadrivov, Ilya V., Hoe Tan, Hark, Jagadish, Chennupati, & Kivshar, Yuri S. (2012). *Appl. Phys. Lett.*, *100*, 121113–4.
[18] d'Alessandro, A., Asquini, R., Trotta, M., Gilardi, G., Beccherelli, R., & Khoo, I. C. (2010). *Appl. Phys. Letts. 97*, iss 9, article #: 093302.
[19] Yanhui *et al.*, & Khoo, I. C. (2012). *Appl. Phys.Letts.* Article # 053119.
[20] Huang, T. J., Liu, Y. J., Yue, B., Liou, J., & Khoo, I. C. (2011). *Journal of Physical Chemistry 115* Iss: 15, 7717–7722.
[21] Ptasinski, Joanna, Kim, Sung W., Pang, Lin, Khoo, I. E., & Fainman, Yeshaiahu (2013). *Optics Letters* Vol. *38*, Iss. 12, 2008–2010
[22] Eichler, H. J. & Macdonald, R. (1991). *Phys. Rev. Lett.*, *67*, 2666–2669.
[23] Khoo, I. C., Lindquist, R. G., Michael, R. R., Mansfield, R. J., & Lopresti, P. (1991). *J. Appl. Phys.*, *69*, 3853.
[24] Khoo, I. C., Park, J. H., & Liou, J. D. (2008). *J. Opt. Soc. Am. B25*, 1931–1937.
[25] See for example, Khoo, I. C., Liou, J., & Stinger, M. V. (2010). *Mole. Cryst. Liq. Cryst.*, *527*, 109–118.
[26] Khoo, I. C., Liou, J., Stinger, M. V., & Zhao, S. (2011). *Mol. Cryst. Liq. Cryst.*, *543*, 151–159.
[27] Khoo, I. C. & Lin, T. H. (2012). *Opt. Lett.*, *37*, 3225–3227.
[28] Chen, Chun-Wei, Jau, Hung-Chang, Wang, Chun-Ta, Lee, Chun-Hong, Khoo, I. C., & Lin, Tsung-Hsien (2012). *Optics Express*, Vol. *20*, No. 21, 23978–23984.
[29] Khoo, I. C., Hong, K. L., Zhao, Shuo, Ma, Ding, & Lin, Tsung-Hsien (2013). *Optics Express* Vol. *21* Issue 4, pp.4319–4327.
[30] Chen, C. W., Jau, H. C., Lee, C. H., Li, C. C., Hou, C. T., Wu, C. W., Lin, T. H., & Khoo, I. C. (2013) *Optical Materials Express*, *3*, Issue: 5, 527–532.
[31] Kikuchi, H., Yokota, M., Hiskado, Y., Yang, H., & Kajiyama, T. (2002). *Nat. Mater.*, vol. *1*, 64–68.
[32] Coles, H. & Pivnenko, M. N. (2005). *Nature*, *436*, 997–1000.
[33] Hisakado, Y., Kikuchi, H., Nagamura, T., & Kajiyama, T. (2005). *Adv. Mater.*, vol. *17*, 96.
[34] Zhibing, G., Gauza, S., Meizi Jiao, J., Xianyu, H., & Wu, S. T. (2009). *Appl. Phys. Letts. 94*, article # (101104).
[35] White, T. J., Bricker, R. L., Natarajan, L. V., Tabiryan, N. V. P., green, L., Li, Q., & Bunning, T. J. (2009). *Adv. Func. Mats.*, *19*, 3484–3488.

[36] Vernon, J. P., Zhao, A. D., Vergara, R., Song, H., Tondiglia, V. P., White, T. J., Tabiryan, N. V., & Bunning, T. J. (2013). *Opt. Exp. 21*, 1645–1655.
[37] Lee, C. R., Lin, J. D., Huang, B. Y., Lin, S. H., Mo, T. S., Huang, S. Y., Kuo, C. T., & Yeh, H. C. (2011). *Opt. Express 19*, 2391–2400.
[38] He, B. Q., Liao, Q., & Huang, Y. (2008). *Opt. Materials 31*, 375–379.
[39] Ferjani, S., Barna, V., De Luca, A., Versace, C., Scaramuzza, N., Bartolino, R., & Strangi, G. (2006). *Appl. Phys. Letts. 89*, 121109.
[40] Hands, P. J. W., Gardiner, D. J., Morris, S. M., Mowatt, C., Wilkinson, T. D., & Coles, H. J. (2011). *Appl. Phys. Lett. 98*, 141102.